

Document downloaded from:

<http://hdl.handle.net/10251/63987>

This paper must be cited as:

Duque, JC.; Patiño Quinchía, JE.; Ruiz Fernández, LÁ.; Pardo Pascual, JE. (2015).
Measuring intra-urban poverty using land cover and texture metrics derived from remote
sensing data. *Landscape and Urban Planning*. 135:11-21.
doi:10.1016/j.landurbplan.2014.11.009.



The final publication is available at

<http://dx.doi.org/10.1016/j.landurbplan.2014.11.009>

Copyright Elsevier

Additional Information

MEASURING INTRA-URBAN POVERTY USING LAND COVER AND TEXTURE
METRICS DERIVED FROM REMOTE SENSING DATA

Juan C. DUQUE (corresponding author)
Research in Spatial Economics (RiSE-group),
Department of Economics,
EAFIT University,
Carrera 49 7 Sur - 50, Medellin, Colombia
e-mail: jduquec1@eafit.edu.co
Phone: (574) 261-9354, Fax: (574) 261-9294

Jorge E. PATINO
Research in Spatial Economics (RiSE-group),
Department of Economics,
EAFIT University,
Carrera 49 7 Sur - 50, Medellin, Colombia
e-mail: jpatinoq@eafit.edu.co

Luis A. RUIZ
Geo-Environmental Cartography and Remote Sensing Group,
Department of Cartographic Engineering, Geodesy and Photogrammetry,
Universitat Politècnica de València,
Camino de Vera, s/n 46022, Valencia, Spain
e-mail: laruiz@cgf.upv.es

Josep E. PARDO-PASCUAL
Geo-Environmental Cartography and Remote Sensing Group,
Department of Cartographic Engineering,
Geodesy and Photogrammetry, Universitat Politècnica de València,
Camino de Vera, s/n 46022, Valencia, Spain
e-mail: jepardo@cgf.upv.es

Abstract

This paper contributes empirical evidence about the usefulness of remote sensing imagery to quantify the degree of poverty at the intra-urban scale. This concept is based on two premises: first, that the physical appearance of an urban settlement is a reflection of the society; and second, that the people who reside in urban areas with similar physical housing conditions have similar social and demographic characteristics. We use a very high spatial resolution (VHR) image from one of the most socioeconomically divergent cities in the world, Medellin (Colombia), to extract information on land cover composition using per-pixel classification and on urban texture and structure using an automated tool for texture and structure feature extraction at object level. We evaluate the potential of these descriptors to explain a measure of poverty known as the Slum Index. We found that these variables explain up to 59% of the variability in the Slum Index. Similar approaches could be used to lower the cost of socioeconomic surveys by developing an econometric model from a sample and applying that model to the rest of the city and to perform intercensal or intersurvey estimates of intra-urban Slum Index maps.

1. Introduction

The majority of the global population today is urban. The percentage of urban dwellers increased from 43% in 1990 to 52% in 2011, and it is expected to grow to 67% by 2050 (United Nations, 2007, 2008, 2012). All population growth from 2011 to 2050 is expected to be absorbed by urban areas, and most of this growth will occur in cities of less developed regions (United Nations, 2012). In developing countries, rapid urban growth normally exceeds the capacity for local governments to deliver services and infrastructure, which increases urban poverty and intra-urban inequalities (Duque et al., 2013).

The monitoring of poverty is a key issue for policy makers because it can help prevent poverty traps and crime nests and allocate public investments where they are needed most (Duque et al., 2013). Urban poverty is a multidimensional phenomenon; as such, there are many ways to measure it. These measures usually include information from at least one of the following dimensions: income/consumption, health/education, and housing (Carr-Hill & Chalmers-Dixon, 2005; Moser, 1998). They are computed from survey or census data, which are quite expensive, time consuming, less frequently produced, and often statistically significant for spatial units that are too large to capture the intra-urban variability of phenomena. This last feature creates inference problems such as the ecological fallacy (I. Baud, Kuffer, Pfeffer, Sliuzas, & Karuppanan, 2010; Robinson, 1950) or aggregation bias (Fotheringham & Wong, 1991; Paelinck & Klaassen, 1979).

This study works toward overcoming these problems by exploring the possibility of using remote sensing imagery to measure urban poverty. This proposal is based on the premise that the physical appearance of a human settlement is a reflection of the society in which it was created and on the assumption that people living in urban areas with similar physical housing conditions have similar social and demographic characteristics (Jain, 2008; Taubenböck et al., 2009). The main advantage of using remote sensing imagery for urban poverty quantification is that this type of data can be obtained faster, at higher frequencies, and for a fraction of the cost required for

field surveys and censuses. Poverty mapping usually follows two types of approaches: the expenditure-based econometric approach linked to a poverty line used by World Bank, and the value-focused approach used by United Nations Development Programme (UNDP) based on the Human Development Index (I. S. A. Baud, Pfeffer, Sridharan, & Nainan, 2009). The Index of Multiple Deprivations (I. Baud, Sridharan, & Pfeffer, 2008), the Slum Index (Weeks, Hill, Stow, Getis, & Fugate, 2007), and the Slum Severity Index (Patel, Koizumi, & Crooks, 2014) all follow the value-focused approach that integrates several dimensions of deprivation in one single measure.

We chose the Slum Index to corroborate this possibility because this measure is based on the physical aspects of dwelling units. A slum household is defined as a group of individuals living under the same roof in an urban area that lacks one or more of the following: durable housing of a permanent nature, sufficient living space (not more than three people sharing the same room), easy access to safe water at sufficient amounts and at an affordable price, access to adequate sanitation in the form of a private or public toilet shared by a reasonable number of people, and security of tenure (UN-Habitat, 2006). Weeks et al. (2007) presented the calculation of the Slum Index from census and survey data as the sum of the fractions of households that lack one or more of the five conditions mentioned above. The value can range from 0, meaning that no slum-like households are present in an area, to 5, where all households in an area lack all five of the features defined by UN-Habitat. The proportion of slum dwellers in cities is strongly correlated with the Human Development Index, which integrates three development indicators: per capita GDP, longevity and educational attainment (UN-Habitat, 2003). Thus, the presence of slums in a city is an indicator of poverty, and the Slum Index is a good proxy variable for urban poverty at the intra-urban level. This paper implements spatial econometric models using data from Medellin (one of the most unequal cities in the world) to assess whether the Slum Index can be estimated using image-derived measures.

Weeks et al. (2007) and Stoler et al. (2012) used land cover descriptors and texture measures from medium to very high spatial resolution satellite imagery to develop spatial econometric

models for predicting the Slum Index as a function of remote sensing-derived variables. This work builds on these previous studies by analyzing a wider set of remote sensing variables on land cover composition, image texture and urban layout spatial pattern descriptors to provide empirical evidence that either supports or refutes the hypothesis that remote sensing could be used to estimate the Slum Index at the intra-urban scale. As our intention was to lower the costs of this approach as much as possible, we use data drawn from an RGB composition of a Quickbird scene with a spatial resolution of 0.60 m captured in May of 2008. The imagery is similar in color and spatial resolution to Google Earth and Microsoft Bing images (Quickbird is a commercial Earth-observation satellite that collects very high spatial resolution -VHR- imagery). Although the conclusions of this exercise may not be valid worldwide, we seek to present new, innovative and low-cost means of measuring urban poverty.

The structure of this paper is as follows: section 2 describes the spatial unit of analysis, the socioeconomic data for Slum Index calculation, the remote sensing data and variables derived from it and the statistical analysis for model specification. The results are presented in section 3, and the subsequent discussion is presented in section 4. Section 5 presents the main conclusions and public policy implications of this line of research for local governments and authorities.

2. Methods

Spatial unit of analysis

Located in the northwestern Colombia (Figure 1), Medellin is the second largest city in Colombia with a population of 2.4 million (DANE, 2012). The urban area of Medellin has two levels of administrative spatial units: communes (16) and neighborhoods (243). The Slum Index is typically reported at the commune level from socioeconomic data available in the Quality of Life Survey (whose sampling process is designed to be representative at this spatial scale). There are two main disadvantages to using communes as the spatial unit of analysis. First, these units are too large for studying the spatial patterns of intra-urban poverty levels. Second, the statistical inference based on large administrative units may be affected by aggregation problems such as

the ecological fallacy (Robinson, 1950) and aggregation bias (Amrhein & Flowerdew, 1992; Fotheringham & Wong, 1991; Paelinck, 2000). In 2007, the average number of surveyed households at the neighborhood level was 84 ± 57 , with values ranging from 3 to 296, and 15.64% of the neighborhoods contained less than 30 surveyed households. Working with such administrative neighborhoods can result in the following three problems: a lack of statistical validity, a small numbers problem for rates calculation (Diehr, 1984), and the potential appearance of spurious spatial autocorrelation (Weeks et al., 2007).

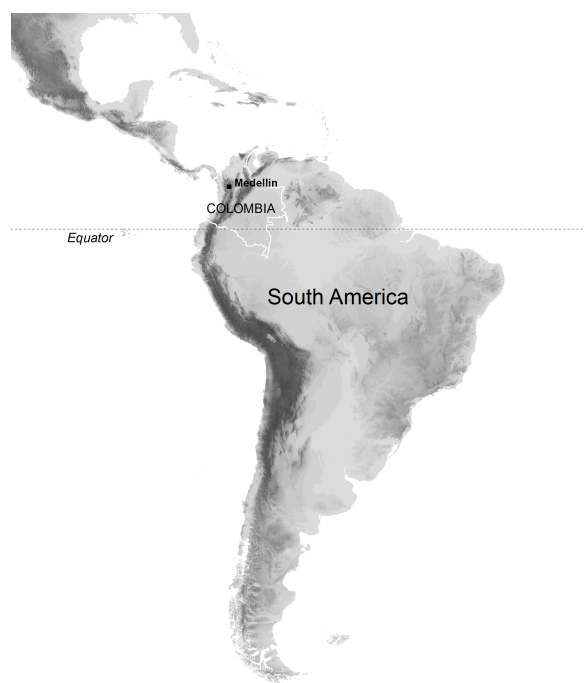


Figure 1. Location of Medellín in Colombia and South America.

An alternative means of addressing the problems described above involves the use of analytical regions, which are spatial units fulfilling specific criteria (e.g., size, shape, attribute homogeneity, among others) that are relevant to the phenomena of study (Duque et al., 2007). Duque et al. (2013) designed analytical regions for the study of intra-urban poverty variations in Medellín. Each analytical region satisfies the following two conditions: it must be homogeneous in terms of socioeconomic characteristics, and it must have at least 100 surveyed households to

ensure statistical validity. These units were delineated by applying the Max-P-Regions algorithm using ClusterPy (Duque et al., 2011; Duque, 2012), which grouped the 243 city neighborhoods into 139 analytical regions. In this paper, we excluded one analytical region at the city's border because it included large portions of unoccupied green spaces that were not part of the urban fabric.

Data

The Slum Index was computed using data from the 2007 Quality of Life Survey of Medellin. This survey includes 184 questions on the following nine dimensions: housing, households, demography, education, social security, income and employment, social participation, gender and family violence, and nutrition. The sample includes 21,861 households that represent 79,912 persons (Duque et al., 2013). Table 1 describes the variables used to calculate the Slum Index and the proportion of housing units in the city existing under these conditions. The proportion of households not connected to piped water or to the sewer system is very low in Medellin because of the city's high coverage of public services, which is atypical of Colombian cities. The proportion of housing units that are constructed from non-durable materials is also very low for this city. Figure 2 shows the Slum Index map at the analytical region level. Slum Index values are highly variable throughout the city, ranging from 0.17 to 0.86, and the map shows a directional spatial pattern with wealthier neighborhoods located in the south and higher values of the Slum Index in the north.

Table 1. Variables used to calculate the Slum Index from the 2007 Quality of Life Survey of Medellin and the proportion of housing units under those conditions. Modified after Duque et al. (2013).

Variable	Description	Dimension	Housing units (%)
Material	Walls are not made of durable material	Housing	0.14
Overcrowding	Three or more persons per room	Households	16.77
Water	Absence of piped water	Housing	0.01
Toilet	Toilet not connected to a sewer	Housing	3.77
Ownership	Residents are not the owners	Households	35.46

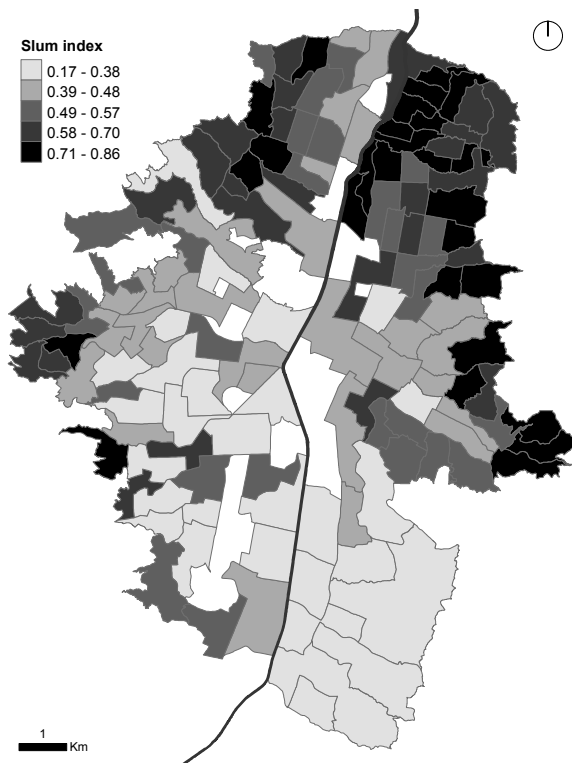


Figure 2. Medellín's Slum Index map at the analytical region level.

We used a VHR image from 2008 to calculate land cover, structure and texture features at analytical region level. We applied two basic image-processing techniques to enhance the information contained in the three color bands: we used principal component analysis to summarize the spectral information contained in the three bands (the first principal component, PC1, explained 98% of the spectral variability contained in the three bands), and we made the band ratios red/blue and green/red to enhance the spectral information for a better differentiation of surfaces that reflected red and green.

Land cover features describe the composition of the urban scene in terms of the amount of basic land cover types (vegetation, soil, and impervious surfaces) and an additional land cover: clay roofs, which quantifies the presence of this roofing material. We used the first principal component (PC1) and both band ratios as inputs to a supervised per-pixel classification to

differentiate the following land cover classes: vegetation, impervious surfaces without clay roofs, soil, water, shadows, and clay roofs. The classification accuracy was assessed using a point-based technique with a reference dataset of randomly selected points (we collected a sample of ground truth points and divided it randomly into two datasets: 80% as the classification training set and 20% as the validation set). Table 2 shows the confusion matrix of this classification. The vegetation, water, impervious surface and clay roofs classes reached producer and user accuracies over 90%, while the shadow and soil classes reached accuracies from 76% to 87%. We then calculated the percentage of each land cover class present in each analytical region to build the land cover features (Figure 3).

Table 2. Accuracy assessment of image classification results.

Ground truth	Vegetation	Impervious surfaces without clay roofs	Water	Shadow	Soil	Clay roofs	Total
Training samples	2952	5636	1732	768	800	2920	14808
Validation samples	738	1409	433	192	200	730	3702
Classified as Vegetation	712	24	0	26	0	14	776
Impervious surfaces without clay roofs	10	1356	6	1	9	0	1382
Water	0	0	400	0	0	0	400
Shadow	6	0	18	165	0	0	189
Soil	10	29	9	0	186	8	242
Clay roofs	0	0	0	0	5	708	713
Total	738	1409	433	192	200	730	
Producer's accuracy (%)	96.48	96.24	92.38	85.94	93.00	96.99	
User's accuracy (%)	91.75	98.12	100.00	87.30	76.86	99.29	
Overall classification accuracy (%)	95.27						
Kappa value	0.94						

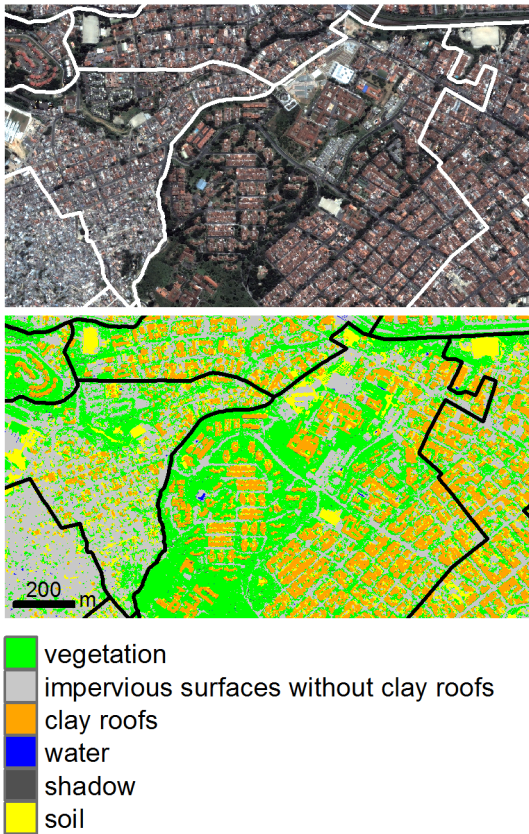


Figure 3. Example of the input VHR image and classified land cover types within analytical regions.

Structural and texture features are abstract variables with great potential to quantitatively differentiate organic, crowded and cluttered spatial patterns from the more structured, ordered and homogeneous urban layouts typical of wealthy neighborhoods. We expected some of these variables to be related to the Slum Index at the analytical region level. The PC1 band and analytical region polygons were entered into the FETEX 2.0 software program, an interactive computer package for image, object-oriented feature extraction (Ruiz, Recio, Fernández-Sarría, & Hermosilla, 2011) to calculate structural and texture variables (FETEX 2.0 is available at the Geo-Environmental Cartography and Remote Sensing Research Group website: <http://cgat.webs.upv.es>).

Structural variables provide information on the spatial arrangement of elements within the polygons in terms of randomness or regularity of the distribution of the elements, and these data were computed in FETEX using the experimental semivariogram approach (Balaguer, Ruiz, Herмосilla, & Recio, 2010; Balaguer-Beser, Ruiz, Herмосilla, & Recio, 2013). The semivariogram is a suitable tool for the quantitative characterization of spatial patterns because it quantifies the spatial associations of the pixel intensity values and measures the degree of spatial correlation between different pixels in an image (Ruiz et al., 2011). Structural features are derived from a zonal analysis defined by a set of singular points on the semivariogram: the first maximum, first minimum, and second maximum. Table 3 shows the description of the ten different structural variables that were calculated using this approach (for a full description of these features see Balaguer et al., 2010; Ruiz et al., 2011).

Texture variables describe the spatial distribution of intensity values in an image and provide information on contrast, uniformity, roughness, etc. (Baraldi & Parmiggiani, 1995). The histogram of pixel values and the Grey Level Co-occurrence Matrix (GLCM) inside each polygon were used for texture feature extraction in FETEX. The histogram is used to compute the kurtosis and skewness features. The GLCM describes the co-occurrences of the pixel values that are separated at a distance of one pixel inside the polygon (Baraldi & Parmiggiani, 1995), and it is used to calculate a set of texture variables proposed by Haralick, Shanmugam, & Dinstein (1973) that are widely used in image processing: uniformity, entropy, contrast, inverse difference moment, covariance, variance, and correlation. The edgeness factor is a feature that represents the density of edges present in a neighborhood (Sutton & Hall, 1972), and FETEX also computes the mean and standard deviation of the edgeness factor within this set of texture features. Table 3 shows the complete list of remote sensing variables used in the statistical analysis.

The VHR image data and image processing methods are the same as those used by Patino, Duque, Pardo-Pascual, & Ruiz (2014) to build a database of remote sensing-derived variables for the study of the relationship between homicide rates and the urban layout in Medellin.

Table 3. Remote sensing-derived variables.

Group	Variable	Description
Land cover features	VEG_P	Percentage of vegetation cover
	IMP_SURF_P	Percentage of impervious surface cover including the clay roof cover
	SOIL_P	Percentage of bare soil cover
	CLAY_ROOFS_P	Percentage of clay roof cover
	F_CLAYR_IMPS	Fraction of clay roof cover over impervious surfaces
Structural features	RVF	Ratio variance at first lag
	RSF	Ratio between semivariance values at second and first lag
	FDO	First derivative near the origin
	SDT	Second derivative at third lag
	MFM	Mean of the semivariogram values up to the first maximum
	VFM	Variance of the semivariogram values up to the first maximum
	DMF	Difference between the mean of the semivariogram values up to the first maximum and the semivariance at first lag
	RMM	Ratio between the semivariance at first local maximum and the mean semivariogram values up to this maximum
	SDF	Second order difference between first lag and first maximum
AFM	Area between the semivariogram value in the first lag and the semivariogram function until the first maximum	
Texture features	SKEWNESS	Skewness value of the histogram
	KURTOSIS	Kurtosis value of the histogram
	UNIFOR	GLCM uniformity
	ENTROP	GLCM entropy
	CONTRAS	GLCM contrast
	IDM	GLCM inverse difference moment
	COVAR	GLCM covariance
	VARIAN	GLCM variance
	CORRELAT	GLCM correlation
	MEAN_EDG	Mean of the edgeness factor
	STDEV_EDG	Standard deviation of the edgeness factor

Model

We developed a model for Slum Index estimation based solely on remote sensing data from a VHR image to assess the performance of the remote sensing-derived variables for this purpose and to examine the associations between urban fabric characteristics and urban poverty. The proposed model has the following general form:

$$\text{Slum Index} = f(\text{land cover}, \text{structure}, \text{texture})$$

We used survey data to compute the Slum Index from socioeconomic variables following the method outlined by Weeks et al. (2007) and a VHR image to extract a wide set of remote sensing-derived measures. Although VHR imagery of higher spectral resolution exists, we deliberately chose to work with an image of a spatial and spectral resolution similar to many aerial color photographs and to Google Earth and Microsoft Bing imagery to make this approach repeatable for analyses of other urban areas around the world. Although the value of the variables that comprise the Slum Index cannot be measured directly from remote sensing data, the spatial characteristics of urban land cover elements can be quantified to serve as a proxy for the Slum Index (Weeks et al., 2007). These characteristics can provide a framework for the analysis of intra-urban variations of poverty so that urban planners and policy makers can identify which areas require the most attention (Stoler et al., 2012).

Stoler et al. (2012), Stow et al. (2007) and Weeks et al. (2007) developed spatial econometric models to estimate the Slum Index in Accra, Ghana, as a function of within-neighborhood measures of vegetation, impervious surface and soil as well as a texture measure from remote sensing imagery. Owen and Wong (2013) reviewed indicators derived from remote sensing imagery and digital elevation data that have been reported to be useful for slum detection. Using information on Guatemala City, the authors found that the variables that best distinguished informal from formal settlements include the entropy of roads, vegetation patch size, vegetation compactness, profile convexity, road density and soil coverage. Following these previous studies, a model for Slum Index estimation using remote sensing imagery should include information on not only land cover materials but also on the spatial pattern of the urban fabric.

Figure 4 outlines the image processing methodology, neighborhood delineation and statistical analysis used to develop the econometric model. The section of the diagram with a gray background portrays the basic steps applied by Duque et al. (2013) that were used to delineate the analytical regions. Due to collinearity among the structural and texture variables, we conducted a factor analysis using the principal components method to consolidate the variables into their main uncorrelated factors. For easier interpretation of factors, we applied Orthogonal

Varimax rotation to maximize the loading of each variable on one factor while minimizing it in others.

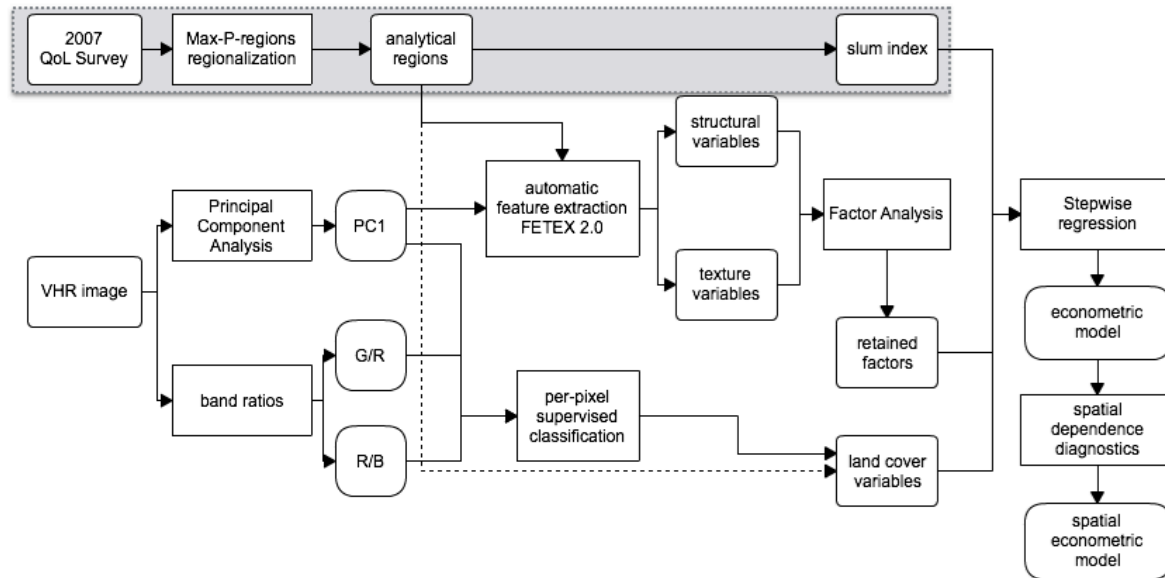


Figure 4. Flow diagram showing the steps for model specification of the Slum Index as a function of remote sensing variables from a VHR image of the urban scene.

As this is the first time that these structural and textural variables have been used to estimate the Slum Index and there is no theoretical model for reference, we used stepwise regression (backward, forward and both) based on the Akaike Information Criterion (AIC) as the variable selection criteria for model specification using R software (R Core Team, 2013) and ran an Ordinary Least Squares (OLS) regression. The use of OLS with spatial data is problematic due to the potential presence of spatial autocorrelation within the model residuals, which violates the assumption of the independence of residuals. We evaluated the OLS residuals for evidence of spatial autocorrelation following the specification search strategy proposed by Florax et al. (2003) and using the Lagrange Multiplier tests and their robust forms to determine the appropriate type of spatial model to use, and we ran the spatially adjusted regression using OpenGeoda software (Anselin et al., 2006). Following the notation of Anselin (1988), the general form of the spatial model is:

$$\text{Slum Index} = X\beta + \rho W \text{Slum Index} + u$$

$$u = \lambda Wu + e$$

where X is an N by K matrix of observations of independent variables (in our case, image derived variables), β is a K by 1 vector of parameters associated with the independent variables, W is a spatial weight matrix that represents the spatial association between regions, ρ is a measure of the strength of that spatial association, and u is the remaining error term with λ being the parameter measuring the strength of the spatial association in the error term. Finally, e is a vector of independently distributed random terms. When neighboring values of the dependent variable have a direct effect on the value of the dependent variable itself, the λ parameter equals zero, and we obtain a spatial autoregressive or spatial lag model. When the spatial dependence enters through the errors rather than through the systematic component of the model, the ρ parameter equals 0, and we obtain a spatial error model.

We first parameterized the spatial weight matrix, which defines the areas that are considered neighbors of a given area, using the Rook and Queen specification of contiguity matrices. The Rook specification states that two polygons are neighbors if they share a border, while the Queen specification states that two polygons are neighbors if they share a border or a vertex. As these specifications created confusing results regarding the type of spatial dependence present in the model, we conducted the specification of a neighbor weight matrix based on a fixed distance band; thus, all neighbors within a specified distance of a given polygon are considered neighbors. To determine an appropriate distance band, we followed the strategy of Troy et al. (2012) and built the semivariogram of the endogenous variable, the Slum Index, to determine the distance at which spatial autocorrelation decays. The semivariogram shows how variance between observations pairs varies as a function of distance, and in this case it showed a terrace-type pattern with a sill at approximately 2 km (Figure 5). This indicated that the autocorrelation of observation pairs leveled off at that distance. We performed a sensitivity analysis using distance

bands ranging from 1.3 to 2 km and found that the models were very consistent in terms of the magnitude and sign of the coefficients. However, the 1.7 km distance band provided conclusive results on the type of spatial model to be used.

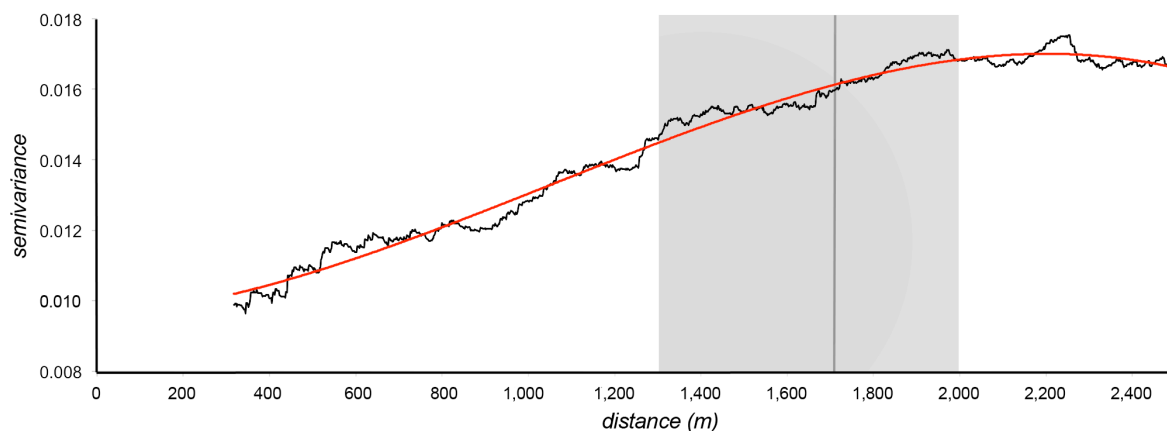


Figure 5. Empirical omnidirectional semivariogram of Slum Index. Smoothed trend line in red. Gray area shows the distance interval tested for the weight contiguity matrix specification.

3. Results

The principal components factor analysis of image structure and texture variables resulted in four retained factors with eigenvalues above 1. These four factors account for 95% of the variance for the original 21 variables. Table 4 shows the rotated factor analysis results. Factor 1 accounts for 57% of the variance among these variables. It was labeled *overall complexity (OC)* as it captures most of the structural variables with the exception of RSF and VFM as well as most of the texture variables with the exception of uniformity, variance and covariance. Factor 2 accounts for 17% of the variance and was labeled *variance* as it captured the texture variables VARIAN and COVAR. The structural variables RSF and VFM were captured by factor 3, which accounts for 15% of the variance. Because RSF pertains to the variability of intensity values at short distances and VFM is related to the variation in changes of the image intensity values as a function of distance (Balaguer et al., 2010), we labeled factor 3 *variation of heterogeneity as a function of the distance (VHD)*. In this context, factor 3 represents the diversity of landscape

elements, and we interpret this factor as a local measure, which complements the global aspects already captured in the OC factor. Factor 4 accounts for 6% of the variance and captured only one texture variable, *uniformity*.

Table 4. Rotated factor loadings (orthogonal Varimax rotation) of image structural and texture variables.

Variable	Factor 1: <i>Overall complexity (OC)</i>	Factor 2: <i>Variance</i>	Factor 3: <i>Variation of heterogeneity as a function of distance (VHD)</i>	Factor 4: <i>Uniformity</i>
RVF	-0.6776	0.5939	0.3585	0.1426
RSF	-0.0613	-0.0453	0.9596	0.0973
FDO	0.9671	-0.0581	-0.2174	-0.0261
SDT	0.8796	0.1118	0.4252	0.0448
MFM	0.9876	0.0837	-0.0453	-0.0570
VFM	-0.2237	0.3901	0.8681	-0.0340
DMF	0.9843	0.1156	0.0218	-0.0617
RMM	-0.6349	0.4211	0.4938	-0.0544
SDF	-0.9806	0.0894	0.1219	0.0143
AFM	0.9950	0.0412	-0.0453	-0.0410
SKEWNESS	0.7958	0.3833	-0.3372	-0.1677
KURTOSIS	-0.7338	-0.5810	0.2399	0.1552
UNIFOR	-0.1785	0.3127	0.0117	0.9072
ENTROP	0.8269	0.1594	-0.2220	-0.4743
CONTRAS	0.9324	-0.0576	-0.3315	-0.0327
IDM	-0.8896	0.0873	0.1759	0.3158
COVAR	0.1014	0.9733	0.0968	0.1397
VARIAN	0.1880	0.9632	0.0654	0.1359
CORRELAT	-0.6808	0.6199	0.3517	0.0299
MEAN_EDG	0.9294	-0.0378	-0.2767	-0.1728
STDEV_EDG	0.7039	0.0208	-0.4758	0.0775

Note: Numbers in bold represent the highest loading of each variable on one factor.

The stepwise regression procedure involves selecting the variables that minimize the model's AIC value through progressive steps, wherein improvements are made to the fitness of the model as each variable is included (forward option) or excluded (backward option) from the initial model. We run stepwise regressions through forward selection, backward elimination and bidirectional elimination using R software and obtained the same results. The variables that were included in the model are the percentage of impervious surfaces (IMP_SURF_P), the fraction of clay roof-cover over impervious surfaces (F_CLAYR_IMPS), the overall complexity factor

(OC), and the variation of heterogeneity as a function of the distance factor (VHD). This linear model yields a multiple R^2 of 0.59 and an adjusted R^2 of 0.58, which indicates that these four variables together can explain up to 58% of the variability of the Slum Index in Medellin. Table 5 shows a summary of the model's parameters estimated using OLS and the results of several tests for the normality of errors, heteroskedasticity and the specification robust test as well as the Lagrange Multiplier tests.

Table 5. Multivariate OLS model of Slum Index as a function of remote sensing variables. Spatial unit: analytical regions. N = 138. Contiguity matrix: 1,700 m distance band, row-standardized weights.

Exogenous variables	Coefficients
Constant	0.900488***
IMP_SURF_P	-0.004223***
F_CLAYR_IMPS	-0.549229***
OC	0.088842***
VHD	-0.030657***
R^2	0.5918
Adjusted R^2	0.5795
Akaike information criterion	-228.949
Schwarz criterion	-214.312
Multicollinearity Condition Number	17
Test on normality of errors: Jarque-Bera test	1.25
Diagnostics for heteroskedasticity: Breusch-Pagan test	1.29
Koenker-Bassett test	1.68
Specification Robust test: White	13.18
Diagnostics for spatial dependence: Lagrange Multiplier – lag	11.07***
Robust LM – lag	4.78**
Lagrange Multiplier – error	6.63***
Robust LM – error	0.35

Note: statistical significance is at the 1, 5 and 10% level as indicated by ***, **, and *, respectively.

The non-significant values of the Breusch-Pagan, Koenker-Bassett and White tests indicate that there was no evidence of heteroskedasticity in the model. The robust version Lagrange Multiplier

tests indicate the presence of spatial autocorrelation in the form of a spatially lagged dependent variable. We adjusted this using a spatial lag model that included the lagged dependent variable (W Slum Index). The highly significant value of the spatial lag variable coefficient indicates that the spatial autocorrelation was properly addressed in the spatial lag model, and a careful examination of the spatial lag model residuals did not show signs of remaining spatial patterns. The Likelihood Ratio test, the AIC and the Schwarz criterion all indicate a better fit of the spatially adjusted regression over its non-spatial counterpart, and the non-significant value of the Breusch-Pagan test again indicates that heteroskedasticity is not present in the spatial model. Table 6 shows the spatial lag model coefficients and the Akaike information criterion, the Schwarz criterion and the results of the Breusch-Pagan test for heteroskedasticity and the Likelihood Ratio test.

Table 6. Spatial Lag model of Slum Index as a function of remote sensing variables. Spatial unit: analytical regions. N = 138. Contiguity matrix: 1,700 m distance band, row-standardized weights.

Exogenous variables	Coefficients
Constant	0.652268***
IMP_SURF_P	-0.003116***
F_CLAYR_IMPS	-0.460770***
OC	0.065046***
VHD	-0.028614***
W Slum index	0.312556***
Pseudo R ²	0.62
Akaike information criterion	-236.098
Schwarz criterion	-218.534
Diagnostics for heteroskedasticity	
Breusch-Pagan test	1.22
Likelihood Ratio test	9.15***

Note: statistical significance is at the 1, 5 and 10% level as indicated by ***, **, and *, respectively.

4. Discussions

We found spillover effects regarding the Slum Index in Medellin, which is in agreement with previous works that have found the same effect for different poverty measures (Duncan et al., 2012; Holt, 2007; Okwi et al., 2007; Orford, 2004; Sowunmi et al., 2012; Voss et al., 2006). The

results of the statistical analysis indicate that the most important remote sensing predictors of the Slum Index at the analytical region level for Medellin include the percentage of impervious surfaces, the fraction of clay roofs over impervious surfaces, the overall complexity factor and the variation of heterogeneity as a function of the distance factor. These variables describe aspects of the land cover composition within the analytical region as well as the spatial pattern of the urban layout in terms of texture and structure.

The model's coefficients indicate a negative association between the Slum Index and the percentage of impervious surfaces, the fraction of clay roof cover over impervious surfaces and the VHD factor. A positive association was found between the Slum Index and the OC factor at the analytical region level. These associations were expected. The Slum Index is higher in the analytical regions with a lower percentage of impervious surfaces. However, this is only the case when the impervious surface is mostly comprised of surfaces other than clay roof and when the urban layout has both higher overall complexity and lower diversity of landscape elements within the analytical region.

The land cover variables such as the percentage of impervious surfaces and fraction of clay roof cover over impervious surfaces are highly significant in both models, which means that the association between roofing materials and urban poverty is present in Medellin. Higher values of the fraction of clay roof over impervious surfaces are related to wealthier neighborhoods in Medellin. This is the case because clay roofs are more expensive to install and maintain than other roofing materials such as industrial roof tiles made from zinc or asbestos and because clay roofs are rarely present in the most deprived areas of the city. However, this does not mean that a house with a different type of roof is more deprived than a house constructed of clay roof tiles. The association that we found holds at the analytical region level, which can include hundreds of houses or buildings. Moreover, the presence and abundance of orange and red clay tile roofs in a city is closely related to its cultural heritage as well as the environmental conditions of each city. This is the case because the characteristics of tile roofs constructed depend on the availability and mineral composition of clays and sands used as the primary source of building materials that

are located within a city's proximity. One can expect that this relationship could be similar in other Latin American cities that share a similar cultural heritage and that also have close access to orange and red clays. Whereas the most important remote sensing predictor of the Slum Index in Accra is the amount of vegetation (Stoler et al., 2012; Weeks et al., 2007), this variable does not perform in the same way for Medellin. In fact, the amount of vegetation is barely related to the Slum Index at the analytical region level for this city with a Pearson's correlation coefficient of 0.14. This may be explained by differences in climate conditions, which influences vegetation abundance in a given location, as well as by cultural differences between the cities' inhabitants.

The structural and texture descriptors that were used to characterize the spatial pattern of the urban layout proved to be useful for Slum Index estimation, and these descriptors are easily computed from VHR imagery and polygon boundary data using FETEX 2.0. The use of image texture measures for Slum Index estimation has been reported for Accra, Ghana (Weeks et al., 2007), and their use for slum detection and mapping has been reported in other different cities around the world such as Campinas and Rio de Janeiro in Brazil (Barros & Sobreira, 2005; P. Hofmann, Strobl, Blaschke, & Kux, 2008); Cape Town, South Africa (Peter Hofmann, 2001); Casablanca, Morocco (Rhinane, 2011); and Ahmedabad, Delhi, Pune and Hyderabad in India (Kit, Lüdeke, & Reckien, 2012; Kohli, Warwadekar, Kerle, Sliuzas, & Stein, 2013; Niebergall, Loew, & Mauser, 2007; Shekhar, 2012). In Medellin, these descriptors indicate that the Slum Index is higher in the analytical regions that registered simultaneously higher overall complexity (OC) and lower variation of heterogeneity as a function of distance (VHD). Figure 6 shows square image tiles of 500 meters in different areas of the city with low and high values of OC and VHD factors. The image tiles are organized according to increasing values of each factor from left to right to show changes in the urban scene as the value of the factors increases. From this figure, the reader can intuitively corroborate the associations of the Slum Index with the OC and VHD values found in the statistical models.

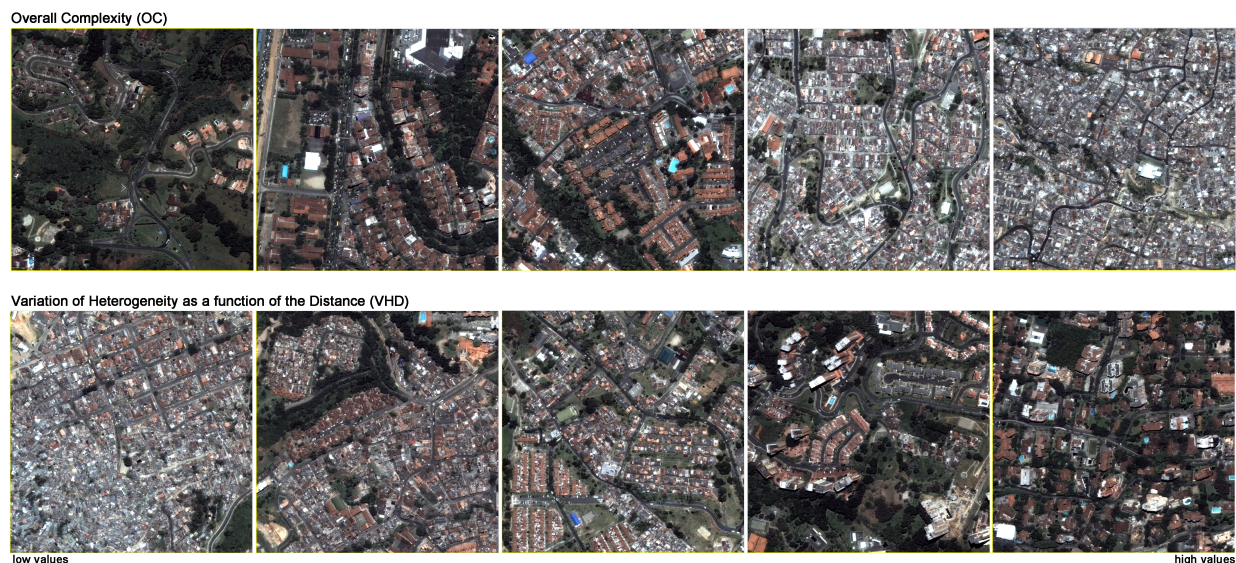


Figure 6. Square image tiles showing urban areas (500 x 500 meters) that have different values of overall complexity (OC) and variation of heterogeneity as a function of distance (VHD) factors. The tiles are organized from left to right according to increasing values of each factor.

High OC values in the image denote that different surface covers exist within close proximity to one another as well as high edge density and high local heterogeneity, which are typical characteristics of the city's most deprived neighborhoods. In these neighborhoods, building density is high, but the dwelling units are rather small with varying roofing materials and located in close proximity to each other. This increases the local heterogeneity and overall complexity of the image. Low overall complexity in the urban layout is associated with analytical regions that have large, homogenous surfaces such as wide roads and avenues, open green spaces, industrial areas that have large buildings with homogeneous roofs and large detached houses surrounded by vegetation. The lowest Slum Index values in this city are located in analytical regions where the existence of large houses surrounded by vegetation is most prevalent. High VHD values are associated with high landscape fragmentation due to a higher diversity of landscape elements. Common examples include residential areas with bigger houses or buildings and the presence of green areas and wide roads surrounded by vegetation, parks, pools, and other urban elements. Low VHD is associated with more crowded and organic urban layouts where small and diverse surfaces exist in close proximity, registering high variability over short distances but lower variance at a higher scale (see Figure 6, VHD tiles).

In Medellin, organic urban layouts are primarily, though not solely, the result of rural-to-urban migration to unplanned urban spaces (Juan C. Duque et al., 2013). Political violence, an ongoing internal armed conflict with guerrillas and paramilitary groups, and the drug war in the rural areas of the country have caused important rural-to-urban migrations in Colombia (Ibáñez & Vélez, 2008). These migrations have impacted urban population growth rates since the mid-20th century in Medellin. Concentrated in the northern periphery of the city, this demographic growth has exceeded the capacity of the local government to deliver services and infrastructure and caused the appearance of slums (Juan C. Duque et al., 2013). The natural population increase combined with structural barriers to socioeconomic advancement, such as poor access to health, education, and work, has also contributed to the perpetuation of slum-like neighborhoods. As these neighborhoods were born from self-build processes without any planning, they are characterized by organic layouts and almost no open spaces. After these areas were consolidated, local authorities provided access to electric energy, piped water, and the sewer system to replace illegal and unsafe electric and water connections while also seeking to decrease losses and increase collection of these services.

We followed the approach of Orford (2004) to assess the usefulness of this model for policy making. We used the local Moran I coefficient, a local indicator of spatial association (Anselin, 1995), to identify areas of concentrated poverty and affluence within the city and to see if the estimated Slum Index from remote sensing can identify the same areas than the survey-based Slum Index. Figure 7 shows a comparison of local Moran's I maps of the survey-based Slum Index versus the estimated Slum Index with the remote sensing-derived variables; both created using OpenGeoda. Although there is not an exact match, the maps show a general good agreement between the High-High and Low-Low areas, which means that the Spatial Lag model is picking the spatial concentration of the poorest and wealthier areas of the city in a rather good way. The Spatial Lag Model residuals are normally distributed, with a mean of 0 and a standard deviation of 0.098. This means that rather than skewing toward low or high values, the model fitted quite well throughout the city.

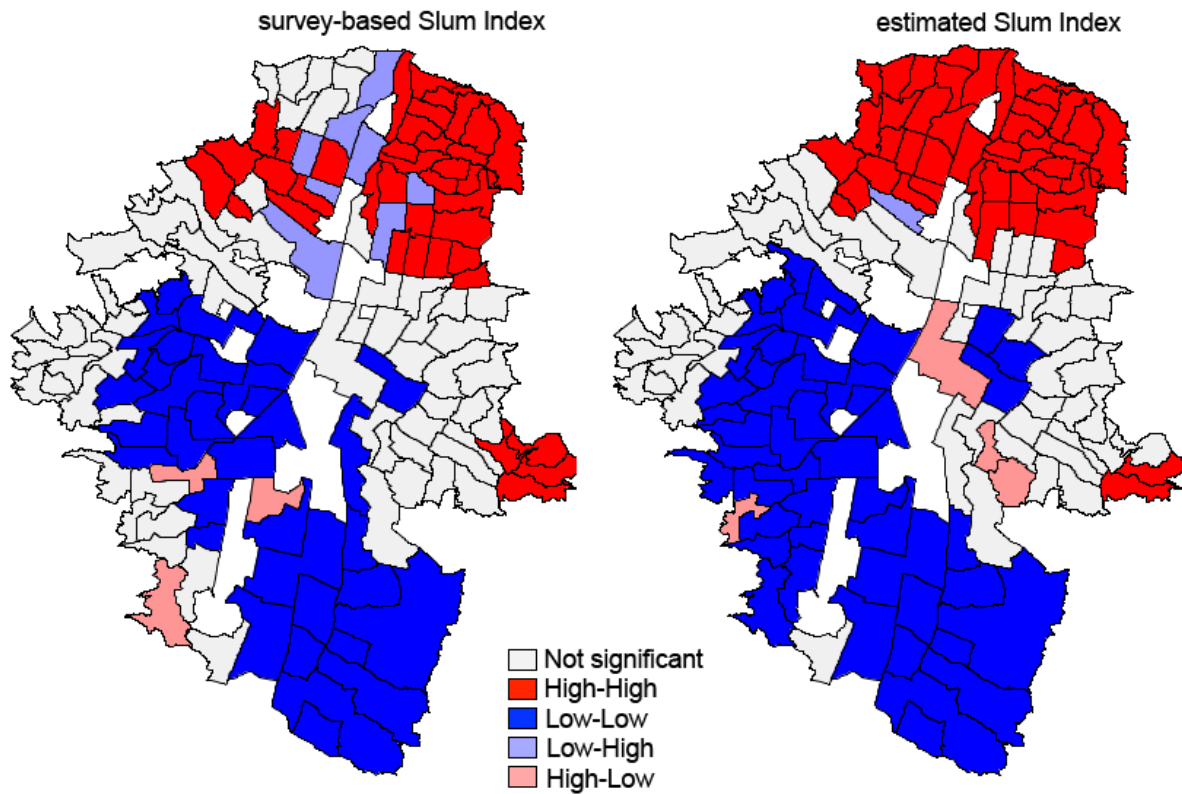


Figure 7. LISA maps of Survey-based vs. estimated Slum Index with remote sensing-derived variables. Spatial clusters of high values, showed in red, indicate areas of concentrated poverty; spatial clusters of low values, showed in blue, indicate areas of concentrated affluence.

5. Conclusions

This paper seeks to estimate the Slum Index for one Latin American city solely using remote sensing data. The usefulness of remote sensing data for estimating the Slum Index at the intra-urban level was previously tested in the case of Accra, Ghana. The findings of the present work corroborate these earlier results in a city with a different geographical and economic setting. In this work, we tested a wider set of remote sensing variables related not only to land cover composition but also to the spatial pattern characteristics of the urban layout.

The presence of spatial autocorrelation with regard to the Slum Index in Medellin indicates that poverty in this city could be tackled through a policy of strategically located investments and programs designed to boost economic development in some of the city's neighborhoods as their outcomes can be expected to affect not only the neighborhoods where the investment is located but surrounding neighborhoods as well. From this point of view, municipal public investments made over the last decade including public library parks and high quality schools seem to be an appropriate strategy for reducing poverty in this city and should be encouraged and improved.

We highlight that the input remote sensing data used in this paper are rather simple. For these data, the most important requirement is a very high spatial resolution to capture the differences in urban layout complexity and heterogeneity. We did not use near-infrared spectral information or other special spectral features from the satellite imagery. The structure and texture variables were calculated from the first principal component band after processing the red, green and blue bands of the color image. Any aerial color image with a very high spatial resolution could serve this purpose. This creates the possibility for rapid Slum Index estimation and intra-urban poverty pattern analysis from remote sensing data given that similar imagery could easily be obtained from Internet services such as Google Earth, Yahoo, or Microsoft Bing Imagery.

The model developed so far for Medellin is based on the city's unique characteristics. Future research should address two main issues: to test whether the same variables relate to intra-urban poverty measures in a similar way in other cities around the world and to verify that this approach provides consistent results over time. When these aspects are resolved, a similar approach could be used for the following purposes in urban settings with sparse socioeconomic data: to lower the cost of socioeconomic surveys by developing an econometric model from a sample and applying that model to the rest of the city and to perform intercensal or intersurveys estimates of intra-urban Slum Index maps.

References

1. Amrhein, C. G., & Flowerdew, R. (1992). The effect of data aggregation on a Poisson regression model of Canadian migration. *Environment and Planning A*, 24(10), 1381–1391. doi:10.1068/a241381
2. Anselin, L. (1995). Local indicators of spatial association - LISA. *Geographical Analysis*, 27(2), 93–115.
3. Anselin, L., Syabri, I., & Kho, Y. (2006). GeoDa: An introduction to spatial data analysis. *Geographical Analysis*, 38(1), 5–22.
4. Balaguer, A., Ruiz, L. A., Hermosilla, T., & Recio, J. A. (2010). Definition of a comprehensive set of texture semivariogram features and their evaluation for object-oriented image classification. *Computers & Geosciences*, 36(2), 231–240. doi:10.1016/j.cageo.2009.05.003
5. Balaguer-Beser, A., Ruiz, L. A., Hermosilla, T., & Recio, J. A. (2013). Using semivariogram indices to analyse heterogeneity in spatial patterns in remotely sensed images. *Computers & Geosciences*, 50, 115–127. doi:10.1016/j.cageo.2012.08.001
6. Baraldi, A., & Parmiggiani, F. (1995). An investigation of the textural characteristics associated with gray level cooccurrence matrix statistical parameters. *IEEE Transactions on Geoscience and Remote Sensing*, 33(2), 293–304. doi:10.1109/36.377929
7. Barros, M., & Sobreira, F. (2005). Analysing spatial patterns in slums: A multiscale approach. In *Congresso Planejamento Urbano Regional Integrado Sustentável - PLURIS*. Sao Carlos.
8. Baud, I., Kuffer, M., Pfeffer, K., Sliuzas, R., & Karuppappan, S. (2010). Understanding heterogeneity in metropolitan India: The added value of remote sensing data for analyzing sub-standard residential areas. *International Journal of Applied Earth Observation and Geoinformation*, 12(5), 359–374. doi:10.1016/j.jag.2010.04.008
9. Baud, I. S. A., Pfeffer, K., Sridharan, N., & Nainan, N. (2009). Matching deprivation mapping to urban governance in three Indian mega-cities. *Habitat International*, 33(4), 365–377. doi:10.1016/j.habitatint.2008.10.024

10. Baud, I., Sridharan, N., & Pfeffer, K. (2008). Mapping Urban Poverty for Local Governance in an Indian Mega-City: The Case of Delhi. *Urban Studies*, 45(7), 1385–1412. doi:10.1177/0042098008090679
11. Carr-Hill, R., & Chalmers-Dixon, P. (2005). *The Public Health Observatory Handbook of Health Inequalities Measurement*. (J. Lin, Ed.) (p. 201). Oxford: The South East Public Health Observatory.
12. Diehr, P. (1984). Small area statistics: large statistical problems. *American Journal of Public Health*, 74(4), 313–4. Retrieved from <http://www.pubmedcentral.nih.gov/articlerender.fcgi?artid=1651496&tool=pmcentrez&rendertype=abstract>
13. Duncan, D. T., Aldstadt, J., Whalen, J., White, K., Castro, M. C., & Williams, D. R. (2012). Space, race, and poverty: Spatial inequalities in walkable neighborhood amenities? *Demographic Research*, 26(17), 409–448. doi:10.4054/DemRes.2012.26.17
14. Duque, J. C., Anselin, L., & Rey, S. J. (2012). The max-p-regions problem. *Journal of Regional Science*, 52(3), 397–419. doi:10.1111/j.1467-9787.2011.00743.x
15. Duque, J. C., Dev, B., Betancourt, A., & Franco, J. L. (2011). ClusterPy: Library of spatially constrained clustering algorithms, Version 0.9.9. RiSE-group (Research in Spatial Economics), EAFIT University. Retrieved from <http://code.google.com/p/clusterpy/>
16. Duque, J. C., Ramos, R., & Suriñach, J. (2007). Supervised regionalization methods: A survey. *International Regional Science Review*, 30(3), 195–220. doi:10.1177/0160017607301605
17. Duque, J. C., Royuela, V., & Noreña, M. (2013). A stepwise procedure to determine a suitable scale for the spatial delineation of urban slums. In E. Fernandez & F. Rubiera Morollón (Eds.), *Defining the spatial scale in modern regional analysis. Advances in Spatial Science* (pp. 237–254). Berlin Heidelberg: Springer-Verlag. doi:10.1007/978-3-642-31994-5_12
18. Florax, R. J. G. M., Folmer, H., & Rey, S. J. (2003). Specification searches in spatial econometrics: the relevance of Hendry's methodology. *Regional Science and Urban Economics*, 33, 557–579. doi:doi:10.1016/S0166-0462(03)00002-4

19. Fotheringham, A. S., & Wong, D. W. S. (1991). The modifiable areal unit problem in multivariate statistical analysis. *Environment and Planning A*, 23(7), 1025–1044. doi:10.1068/a231025
20. Haralick, R. M., Shanmugam, K., & Dinstein, I. (1973). Textural features for image classification. *IEEE Transactions on Systems, Man, and Cybernetics*, SMC-3(6), 610–621.
21. Hofmann, P. (2001). Detecting informal settlements from IKONOS image data using methods of object oriented image analysis-an example from Cape Town (South Africa). *Jürgens, C.(Ed.): Remote Sensing of Urban Areas/ ...*, 107–118. Retrieved from http://www.ecognition.com/sites/default/files/395_hofmann.pdf
22. Hofmann, P., Strobl, J., Blaschke, T., & Kux, H. J. H. (2008). Detecting informal settlements from QuickBird data in Rio de Janeiro using an object-based approach. In T. Blaschke, S. Lang, & G. J. Hay (Eds.), *Object-based image analysis - Spatial concepts for knowledge-driven remote sensing applications*. (pp. 531–553). New York: Springer.
23. Holt, J. B. (2007). The topography of poverty in the United States: a spatial analysis using county-level data from the Community Health Status Indicators project. *Preventing Chronic Disease*, 4(4), 1–9. Retrieved from <http://www.pubmedcentral.nih.gov/articlerender.fcgi?artid=2099276&tool=pmcentrez&rendertype=abstract>
24. Ibáñez, A. M., & Vélez, C. E. (2008). Civil conflict and forced migration: The micro determinants and welfare losses of displacement in Colombia. *World Development*, 36(4), 659–676. doi:10.1016/j.worlddev.2007.04.013
25. Jain, S. (2008). Remote sensing application for property tax evaluation. *International Journal of Applied Earth Observation and Geoinformation*, 10(1), 109–121. doi:10.1016/j.jag.2007.10.008
26. Kit, O., Lüdeke, M., & Reckien, D. (2012). Texture-based identification of urban slums in Hyderabad, India using remote sensing data. *Applied Geography*, 32(2), 660–667. doi:10.1016/j.apgeog.2011.07.016

27. Kohli, D., Warwadekar, P., Kerle, N., Sliuzas, R., & Stein, A. (2013). Transferability of Object-Oriented Image Analysis Methods for Slum Identification. *Remote Sensing*, 5(9), 4209–4228. doi:10.3390/rs5094209
28. Moser, C. O. N. (1998). The Asset Vulnerability Framework : Reassessing Urban Poverty Reduction Strategies. *World Development*, 26(1), 1–19.
29. Niebergall, S., Loew, A., & Mauser, W. (2007). Object-oriented analysis of very high-resolution QuickBird data for mega city research in Delhi, India. In IEEE (Ed.), *2007 Urban Remote Sensing Joint Event* (pp. 0–7). Paris, France: IEEE.
30. Okwi, P. O., Ndeng'e, G., Kristjanson, P., Arunga, M., Notenbaert, A., Omolo, A., ... Owuor, J. (2007). Spatial determinants of poverty in rural Kenya. *Proceedings of the National Academy of Sciences of the United States of America*, 104(43), 16769–16774. doi:10.1073/pnas.0611107104
31. Orford, S. (2004). Identifying and comparing changes in the spatial concentrations of urban poverty and affluence: a case study of inner London. *Computers, Environment and Urban Systems*, 28(6), 701–717. doi:10.1016/j.compenvurbsys.2003.07.003
32. Owen, K. K., & Wong, D. W. (2013). An approach to differentiate informal settlements using spectral, texture, geomorphology and road accessibility metrics. *Applied Geography*, 38, 107–118. doi:10.1016/j.apgeog.2012.11.016
33. Paelinck, J. H. P. (2000). On aggregation in spatial econometric modelling. *Journal of Geographical Systems*, 2(2), 157–165. doi:10.1007/PL00011452
34. Paelinck, J. H. P., & Klaassen, H. (1979). *Spatial econometrics*. Farnborough, UK: Saxon House.
35. Patel, A., Koizumi, N., & Crooks, A. (2014). Measuring slum severity in Mumbai and Kolkata: A household-based approach. *Habitat International*, 41, 300–306. doi:10.1016/j.habitatint.2013.09.002
36. Patino, J. E., Duque, J. C., Pardo-Pascual, J. E., & Ruiz, L. a. (2014). Using remote sensing to assess the relationship between crime and the urban layout. *Applied Geography*, 55, 48–60. doi:10.1016/j.apgeog.2014.08.016

37. R Core Team. (2013). R: A language and environment for statistical computing. Vienna, Austria. URL <http://www.R-project.org/>. Retrieved from <http://www.r-project.org/>
38. Rhinane, H. (2011). Detecting slums from SPOT data in Casablanca Morocco using an object based approach. *Journal of Geographic Information System*, 03(03), 209–216. doi:10.4236/jgis.2011.33018
39. Robinson, W. S. (1950). Ecological correlations and the behavior of individuals. *American Sociological Review*, 15(3), 351–357.
40. Ruiz, L. A., Recio, J. A., Fernández-Sarría, A., & Hermosilla, T. (2011). A feature extraction software tool for agricultural object-based image analysis. *Computers and Electronics in Agriculture*, 76(2), 284–296. doi:10.1016/j.compag.2011.02.007
41. Shekhar, S. (2012). Detecting slums from Quick Bird data in Pune using an object oriented approach. *International Archives of the Photogrammetry, Remote Sensing and Spatial Information Sciences*, XXXIX(B8), 519–524.
42. Sowunmi, F. A., Akinyosoye, V. O., Okoruwa, V. O., & Omonona, B. T. (2012). The Landscape of Poverty in Nigeria: A Spatial Analysis Using Senatorial Districts- level Data. *American Journal of Economics*, 2(5), 61–74. doi:10.5923/j.economics.20120205.01
43. Stoler, J., Daniels, D., Weeks, J. R., Stow, D. a., Coulter, L. L., & Finch, B. K. (2012). Assessing the utility of satellite imagery with differing spatial resolutions for deriving proxy measures of slum presence in Accra, Ghana. *GIScience & Remote Sensing*, 49(1), 31–52. doi:10.2747/1548-1603.49.1.31
44. Stow, D., Lopez, A., Lippitt, C., Hinton, S., & Weeks, J. R. (2007). Object-based classification of residential land use within Accra, Ghana based on QuickBird satellite data. *International Journal of Remote Sensing*, 28(22), 5167–5173. doi:10.1080/01431160701604703
45. Sutton, R. N., & Hall, E. L. (1972). Texture Measures for Automatic Classification of Pulmonary Disease. *IEEE Transactions on Computers*, C-21(7), 667–676. doi:10.1109/T-C.1972.223572
46. Taubenböck, H., Wurm, M., Setiadi, N., Gebert, N., Roth, A., Strunz, G., ... Dech, S. (2009). Integrating remote sensing and social science - The correlation of urban

- morphology with socioeconomic parameters. In IEEE (Ed.), *2009 Urban Remote Sensing Joint Event*. London.
47. Troy, A., Grove, J. M., & O'Neil-Dunne, J. (2012). The relationship between tree canopy and crime rates across an urban rural gradient in the greater Baltimore region. *Landscape and Urban Planning*, *106*, 262–270.
 48. UN-Habitat. (2003). *Slums of the World: the face of urban poverty in the new millennium? UN-Habitat, Nairobi* (pp. 1–91). Retrieved from <http://www.unhabitat.org/pmss/listItemDetails.aspx?publicationID=1124>
 49. UN-HABITAT. (2006). *State of the World's Cities 2006/7* (p. 204). UN-HABITAT. Retrieved from http://www.unhabitat.org/documents/media_centre/sowcr2006/sowcr5.pdf
 50. United Nations. (2007). World urbanization prospects: The 2007 revision. Retrieved July 30, 2011, from <http://www.un.org/esa/population/publications/wup2007/2007wup.htm>
 51. United Nations. (2008). *Urban population, development and the environment 2007*. New York.
 52. United Nations. (2012). *World Urbanization Prospects: The 2011 Revision* (p. 50). New York. Retrieved from http://esa.un.org/unpd/wup/pdf/WUP2011_Highlights.pdf
 53. Voss, P. R., Long, D. D., Hammer, R. B., & Friedman, S. (2006). County child poverty rates in the US: a spatial regression approach. *Population Research and Policy Review*, *25*(4), 369–391. doi:10.1007/s11113-006-9007-4
 54. Weeks, J. R., Hill, A. G., Stow, D., Getis, A., & Fugate, D. (2007). Can we spot a neighborhood from the air? Defining neighborhood structure in Accra, Ghana. *GeoJournal*, *69*(1-2), 9–22. doi:10.1007/s10708-007-9098-4